BNL-108315-2015-JA

Single to multiparticle states in $CeRhIn_5$ probed with neutron scattering

C. Stock,[1] J. A. Rodriguez-Rivera,[2,3] K. Schmalzl,[4] E. E. Rodriguez,[5] A, Stunault,[6] and C. Petrovic[7]

[1] *School of Physics and Astronomy, University of Edinburgh, Edinburgh EH9 3JZ, UK*
[2] *NIST Center for Neutron Research, National Institute of Standards and Technology, 100 Bureau Dr., Gaithersburg, MD 20889*
[3] *Department of Materials Science, University of Maryland, College Park, MD 20742*
[4] *Julich Centre for Neutron Science, Forschungszentrum Julich, Outstation at Institut Laue-Langevin, Boite Postale 156, 38042 Grenoble Cedex 9, France*
[5] *Department of Chemistry of Biochemistry, University of Maryland, College Park, MD, 20742, U.S.A.*
[6] *Institute Laue-Langevin, B. P. 156, 6 rue Jules Horwitz, F-38042 Grenoble Cedex 9, France*
[7] *Department of Physics, Brookhaven National Laboratory, Upton, New York, 11973, USA*

(Dated: July 28, 2014)

Neutron scattering is used to measure the quantum spin fluctuations in $CeRhIn_5$ - the parent material of the $CeXIn_5$ superconducting series. Out-of-plane spin fluctuations are gapped and localized in momentum, similar to the spin excitons in $CeCoIn_5$. The in-plane fluctuations consist of sharp spin-wave excitations parameterized by a nearest neighbor exchange J_{RKKY}=0.88 ± 0.05 meV that crossover to a temporally and spatially broad multiparticle spectrum with energies of $\sim 2 \times J_{RKKY}$. This continuum represents composite fluctuations that illustrate the breakdown of single magnons originating from the delicate energy balance between localized $4f$ and itinerant behavior in a heavy metal. The experiment therefore shows how quasiparticle behavior is changed by the close proximity of quantum criticality.

The description of physical systems in terms of composite states has provided the basis for a number of theories in the physical sciences. Analogies have been drawn with high-energy physics, and in particular quantum chromodynamics, where fundamental particles are composed of quarks with fractional quantum numbers. [1, 2] In optical physics, dressed states are used as a basis to understand molecular - light interactions. [3] In unconventional and high temperature superconductors, a resonating valence bond state has been proposed where fermionic $S = \frac{1}{2}$ spins pair up to form a net $S_{effective}$=1 object. [4] Composite charge and spin states, such as Zhang-Rice singlets or spinon-holons, have also been suggested to be fundamental to superconductivity, frustrated magnetism, and even quantum criticality. [5–9] Here we use neutron scattering to demonstrate that in $CeRhIn_5$, an antiferromagnetic parent heavy fermion located near a quantum critical transition to superconductivity, the underlying excitations show a strong fractional character and we directly observe the breakdown of these composite quasiparticles with neutron scattering.

$CeRhIn_5$ is a heavy fermion metal, part of the $CeTIn_5$ (T=Rh, Ir, and Co) intermetallic series displaying an interplay between antiferromagnetism and superconductivity. The presence of two-dimensional layers of Ce^{3+} ions connects the physics of these systems with other unconventional superconductors like the cuprates [10–12] or iron based pnictide/chalcogenide superconductors. [13–15] $CeRhIn_5$ magnetically orders at T_N=3.8 K [16–18] and enters an unconventional superconducting phase which can be accessed either at very low temperatures of $\sim$ 75 mK or through hydrostatic pressure. [19, 20] The magnetic and electronic properties have been found to be intertwined with heat and electrical transport properties displaying an electronic scattering rate proportional to the magnetic entropy. [21]

$CeRhIn_5$ is isostructural with $CeCoIn_5$ which is superconducting at ambient pressures with a T_c=2.3 K. The order parameter of the superconducting phase has a d-wave symmetry with nodes in the ab plane. [22, 23] Magnetism and superconductivity are strongly coupled as evidenced by neutron scattering measurements reporting a doublet spin-resonance peak connected with superconductivity and indicating an order parameter that changes sign, consistent with d-wave symmetry. [24, 25] The c-axis polarized magnetic fluctuations in $CeCoIn_5$ were found to peaked near the commensurate $(\frac{1}{2}, \frac{1}{2}, \frac{1}{2})$ point indicating antiferromagnetic spin correlations both within the ab plane and along c. The condensation of these spin excitons was suggested to be responsible for the "Q-phase" reported to exist in the superconducting phase at magnetic fields near H_{c2}. [26, 27] Antiferromagnetic $CeRhIn_5$ provides an opportunity to study the low temperature spin fluctuations in proximity of a quantum phase transition to superconductivity in the clean limit.

Neutron measurements were performed at NIST (Gaithersburg, USA) using MACS and at the ILL (Grenoble, France) using the IN12 spectrometer and the D23 and D3 diffractometers. The samples were aligned in the HHL scattering plane and were prepared using self-flux method. [28] Given the strong effect of absorption, the experiments and analysis have been guided by a finite element analysis. Further details are provided in the supplementary information.

We first review the magnetic structure in the antiferromagnetic phase (T_N=3.8 K) studied with polarized neutrons. There are two irreducible representations for the space group $P4/mmm$ with magnetic ordering wavevector $\mathbf{q_0}$=(0.5,0.5,α); τ_2 which has two basis vectors ($\psi_{2,3}$) along [100] and [010] and τ_1 with ψ_1 along [001].

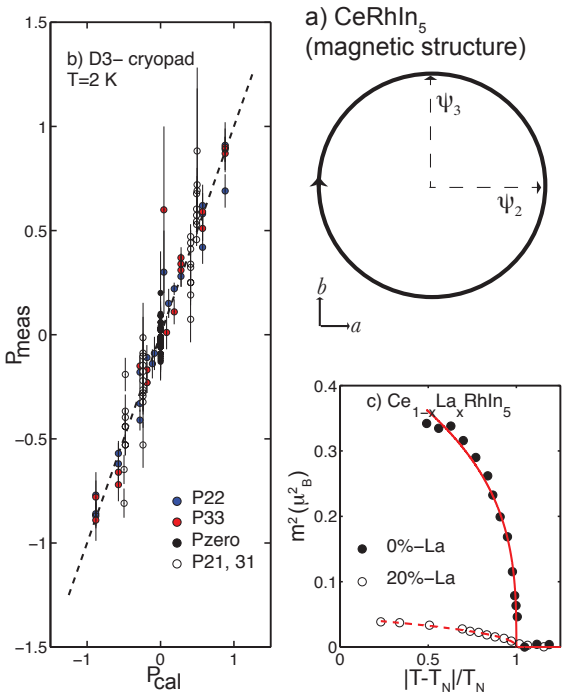

FIG. 1. The magnetic structure of $CeRhIn_5$ investigated using spherical polarimetry (cryopad-D3). *a*) illustrates the magnetic structure based upon spherical polarimetry in terms of the basis vectors $\psi_{2,3}$ described in the text. *b*) a plot of $P_{measured}$ as a function of $P_{calculated}$ based upon an isotropic spiral model described in *a*). *c*) shows a plot of the magnetic order parameter (D23) for both pure $CeRhIn_5$ (T_N=3.7 ± 0.1 K) and 20% La doped (T_N=2.2 ± 0.2 K). The plot is based upon 10 different magnetic magnetic bragg peak positions.

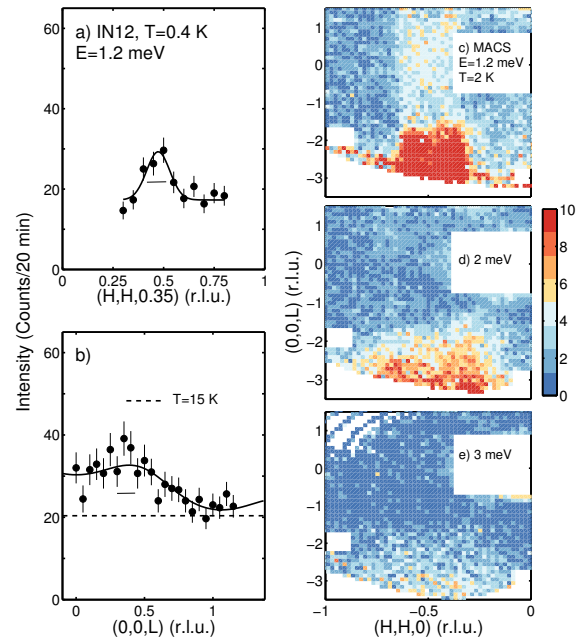

FIG. 2. Constant energy scans taken on IN12 and MACS in the antiferromagnetic phase. $a-b$) illustrate fluctuations polarized along c with the horizontal bar being the spectrometer resolution. $c-e$) show constant energy slices showing the energy dependence of the spin fluctuations. Fluctuations at large L characteristic of in-plane fluctuations are present to high energy transfers. The solid lines are absorption and resolution corrected fits described in the main text.

Figure 1 summarizes diffraction data from D3 (ILL) using spherical polarimetry (cryopad) at T=2 K and D23 (ILL) with unpolarized neutrons. The magnetism is characterized by an incommensurate Bragg peak $\mathbf{Q}$=(0.5,0.5,0.297) allowing polarization intensities to be readily measured. [29] Spherical polarimetry is ideal for studying this problem given the magnetic Ce^{3+} ions occupy a primitive tetragonal lattice where unpolarized diffraction is not able to uniquely distinguish chiral magnetism from a spin density wave (a similar problem was discussed in [30]). Fig. 1 *b*) plots $P_{measured}$ agains $P_{calculated}$ assuming a perfect $a-b$ spiral with $\mathbf{M} = \mathbf{M}_a + i\mathbf{M}_b$ (with $|\mathbf{M_a}| = |\mathbf{M_b}|$). Such a magnetic structure gives a polarization matrix with off diagonal elements $P_{21,31} = \eta\frac{M_y M_z}{M^2}$, where η is the domain population difference given by ($\eta \equiv \frac{V_+ - V_-}{V_+ + V_-}$, with $V_\pm$ the volume fractions of the two ± chiral domains), and diagonal elements $P_{22,33} = \frac{M_y^2 - M_z^2}{M^2}$.

We observe a nonzero off diagonal component $P_{21,31}$ indicating a chiral magnetic structure with a net domain imbalance. Symmetry consideration would imply two domains with a vector chirality pointing along ± [001] and Fig. 1 *b*) is fitted with a domain population of η=0.68 ± 0.05, likely the result of strain and sample geometry. This domain preference allows us to uniquely identify the structure as a spiral over a spin density wave. Fig. 1 *b*) is a fit to all nonzero matrix elements using only the τ_2 irreducible representation with equal components of the two basis vectors (magnetic structure illustrated in Fig. 1 *a*). No detectable *c*-axis component of the moment was found indicating the absence of basis vectors from τ_1.

The involvement of only τ_2 in the phase transition is consistent with T_N being second order predicted by Landau theory (Fig. 1 *c*)). [31, 32] Pure $CeRhIn_5$ was measured to have a critical exponent of β=0.15 ± 0.02, similar to other 2D Heisenberg systems, namely K_2MnF_4. [33] On doping with La, both T_N [17, 34] and the ordered moment are suppressed (Fig. 1 *c*) and β increases to 0.25 ± 0.03 as expected for the critical properties near a tricritical point. The critical exponent presumably reflects the line of quantum phase transitions that separate the antiferromagnetic from the superconducting phase in pressure and temperature. [35]

We now discuss the inelastic scattering probing the spin dynamics. Fig. 2 illustrates a summary of constant

energy scans taken on IN12 and MACS. Fig. 2 a) shows an in-plane momentum scan finding the magnetic scattering to be peaked at (0.5,0.5) indicating antiferromagnetic correlations within the $a-b$ plane. Fig. 2 b) shows a scan along the [001] direction finding momentum broadened correlations which decay with L. The solid line is a fit to $I(\mathbf{Q}) \propto f(Q)^2 \times [1-(\hat{\mathbf{Q}}\cdot\hat{\mathbf{c}})^2]\sinh(c/\xi_c)/[\cosh(c/\xi_c)+\cos(\mathbf{Q}\cdot\mathbf{c})]$ which represents short-range antiferromagnetically correlated Ce^{3+} moments polarized along c with a dynamic correlation length ξ_c. $f(Q)^2$ is the magnetic form factor. [36] The dynamic correlation length was derived to be ξ_c= 3.1 ±0.7 Å indicating little coupling between the Ce^{3+} layers.

Fig. 2 $c-e$) illustrate full constant energy maps taken on MACS at energy transfers of 1.2-3 meV ($c-e$). Panel c) illustrates that, as well as the magnetic scattering near L=0 from the out of plane fluctuations (discussed above), strong scattering is also present at large L indicative fluctuations polarized within the ab plane. The scattering diminishes rapidly with temperature confirming the magnetic nature (see supplementary information). We note that the scattered energy transfer is significantly less than the first crystal field excitation at ∼ 7-9 meV, indicating that the transition results from excitations within the Ce^{3+} ground state doublet. [37] The correlated scattering is present at higher energies as evidenced by similar scans in d) and e). Interestingly, while the in-plane fluctuations (at large L) persist up to high energy transfers, the out of plane fluctuations (near $L=0$) are localized to low-energy transfers.

Having established the presence of c-axis polarized fluctuations (near L=0 in Fig.2 $a-b$) and in-plane fluctuations (observed at large L in Fig. 2 $c-e$), we now discuss the energy dependence. Fig. 3 a) shows constant $\vec{Q}$=(0.5,0.5,0.3) scans taken in the antiferromagnetic phase (T=0.4 K) where a well defined gapped excitation is observed which is broader than the experimental resolution. An antisymmetric lorentzian fit gives a peak energy position of $\hbar\Omega$=1.21 ± 0.06 meV and line width (half-width) of $\hbar\Gamma$=0.22 ± 0.14 meV. Similar to the spin resonance in $CeCoIn_5$, the c axis polarized fluctuations are therefore gapped in the antiferromagnetic phase as well as localized in momentum and energy. These same c-axis polarized fluctuations presumably persist in the presence of superconductivity and form the doublet spin resonance in $CeCoIn_5$.

Fig. 3 c) displays a constant Q slice (integrating over L=[-1.5,-4]) sensitive to the in-plane scattering. Sample one-dimensional cuts through the data are shown in Fig. 4. The false color plot shown in Fig. 3 c) displays sharp dispersing low-energy fluctuations and a higher energy continuum. To extract a dispersion, we have fit constant energy scans (examples shown in Fig. 4 $a-c$) to gaussians symmetrically displaced from the $\vec{Q}$=($\frac{1}{2}$,$\frac{1}{2}$) and illustrated by the open circles in Fig. 3 c). The constant

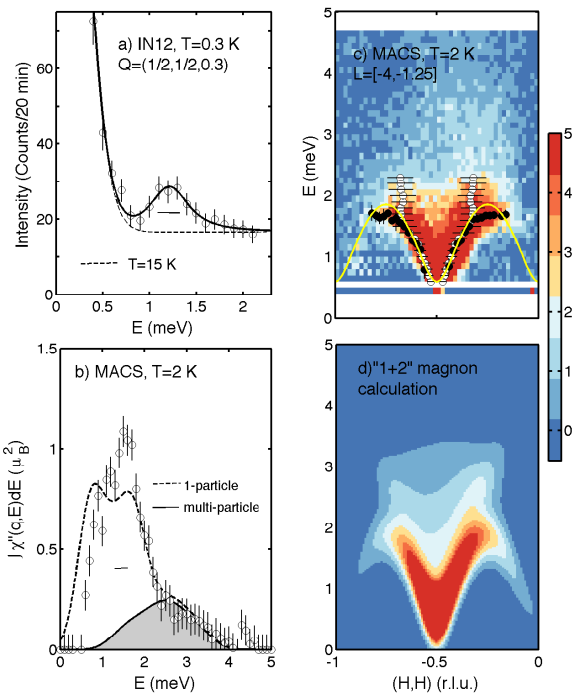

FIG. 3. Constant-Q scans taken on IN12 and MACS. a) illustrate the energy dependence of the out of plane c axis polarized spin fluctuations. c) shows a constant-Q slice taken on MACS (integrating over L=[-4,-1.25]) with the solid points fits to constant-Q scans and the open circles fits to constant energy. A strong continuum of magnetic fluctuations is present above the top of the 1-magnon band. c) shows a resolution and absorption corrected calculation considering single and multiparticle states with the momentum integrated intensities plotted in d) and compared with experiment.

energy fits show dispersing excitations at wave vectors close to ($\frac{1}{2}$,$\frac{1}{2}$), but at the zone boundary near ($\frac{1}{4}$, $\frac{1}{4}$) the "dispersion" becomes nearly vertical.

Representative constant Q scans are shown in Fig. 4 $d-f$. Two damped harmonic oscillators convolved with the resolution were used to describe the low-energy nearly resolution limited excitation and the broad continuum of scattering at higher energies. The sharp excitation energy positions are denoted by the filled points in Fig. 3. To extract an estimate for the localized J_{RKKY} exchange, we have fit the peak locations of the sharp component to the dispersion for a $j_{eff}=\frac{1}{2}$ "spins" (capturing the doublet nature of the ground state) on a square lattice. The problem has been studied in the purely classic $S=\frac{5}{2}$ limit in Rb_2MnF_4 where $E(\vec{q}) = 2J_{RKKY}\sqrt{\alpha^2-\gamma(\vec{q})^2}$, with $\gamma(\vec{q}) = \cos[\pi(H+K)]\cos[\pi(-K+H)]$. Based on the fit in Fig. 3, we extract J_{RKKY}=0.88 ± 0.05 meV and an anisotropy α=1.06 ± 0.02 meV.

Having described the sharp component, we now discuss

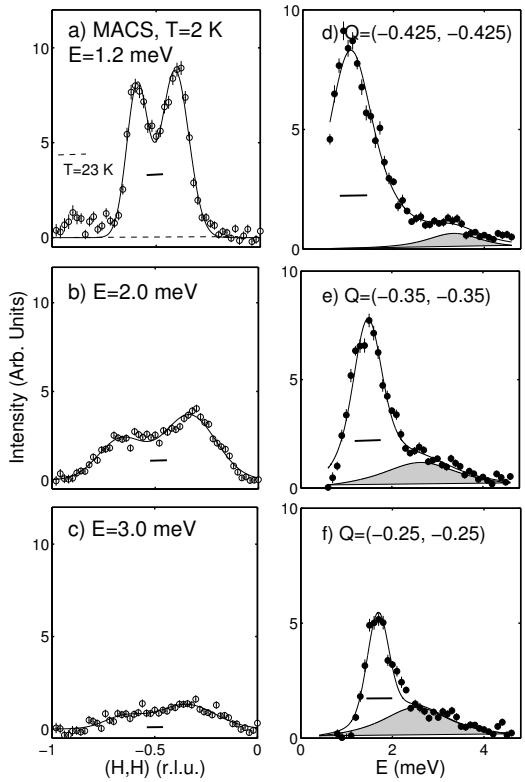

FIG. 4. Constant energy $(a-c)$ and Q $(d-f)$ cuts through the MACS data. The solid lines in $a-c$ are to gaussians displaced from the commensurate $(\frac{1}{2}, \frac{1}{2})$ position. Solid lines in $d-f$ are fits to damped harmonic oscillators as discussed in the text. The shaded region is the component originating from multiparticle excitations. $d-f$ are integrated over $\pm(0.025, 0.025)$.

the broad continuum at higher energies. This continuum extends up to about twice the top of the band described by the sharp excitation. Given that the scattering is reminiscent of two-magnon scattering in localized (and insulating) chains and ladders, [1, 38, 39] we have calculated the multiparticle two-magnon scattering cross section following theories applied to describe quantum fluctuations in Rb_2MnF_4 where the classical $S = \frac{5}{2}$ imposes a very weak continuum. [40, 41] Fig. 3 *b*) shows a plot of the calculation with the one-magnon term superimposed to give the sharp component hence we have referred to this as the "1+2" model. The momentum integrated intensity from the calculations is over plotted in Fig. 3 *b*). The "1-magnon" component fails at low energy transfers, likely due experimental limitations owing to resolution and the elastic line dominated by incoherent nuclear scattering.

Several features are reproduced in the multiparticle calculation: first, the broad continuum of scattering which extends up to nearly $2\times J_{RKKY}$; and second, the nearly vertical columns of scattering which extend up in energy near the zone boundary. Such continuum have been notably observed in one-dimensional chains and originate from spinons with a fermion character as opposed to conventional spin fluctuations which are described by bosons. Near the magnetic zone boundary, as illustrated in Fig. 4, the two components can be separated with both accounting for roughly equal amounts in terms of the integrated intensity. When all of the scattering is integrated over the magnetic Brillouin zone, the total spectral weight (accounting for absorption) is estimated at 1.7 ± 0.5 μ_B^2 to be compared with 1.9 μ_B^2 expected based upon a single ion crystal field analysis. The experiment therefore captures all of the low-energy spectral weight once the multiparticle component is included.

It is interesting to compare the excitation spectrum observed here with results in the cuprate and iron based superconductors close to the hole doped superconducting transition. The strong continuum described above contrasts with localized S=$\frac{1}{2}$ La_2CuO_4 where most of the spectral weight comprises a sharp in energy one-magnon cross section. [42] Our experiment observes the break up of composite states characterized by the sharp harmonic excitations to dressed multi particle states at higher energies. While the observation of both sharp excitations and a higher-energy continuum is relatively unique in $CeRhIn_5$, it is possible that similar physics carries over to strongly correlated cuprates and iron based superconductors and predictions have been made for two dimensional model magnets. [43] $Fe_{1+x}Te$ also displays nearly vertical rods of scattering near the zone boundary. [44] $YBa_2Cu_3O_{6.35}$ (located near the hole doped boundary of high temperature superconductivity and antiferromagnetism), displays a broadening and loss of spectral weight for fluctuations near the magnetic zone boundary and this has been connected with the charge pseudogap phase notably found with optical techniques and NMR. [45–47] Similar anomalous dispersions, though with much less spectral weight, near the zone boundary have been reported in insulating La_2CuO_4. [48]

In summary, we have studied the magnetic structure and excitations in chiral $CeRhIn_5$. We have confirmed the in plane spiral magnetism through the use of spherical polarimetry. The magnetic excitations are found to consist of both c axis polarized and in plane polarized fluctuations. The c axis fluctuations are localized in momentum and energy while the in plane fluctuations consist of both a sharp dispersing component and a broad continuum of scattering reminiscent of multi particle cross sections observed in low dimensional magnets. This therefore illustrates the composite nature of the low energy fluctuations in a heavy metal near quantum criticality.

This work was funded by the Carnegie Trust for the Universities of Scotland, the Royal Society of Edinburgh, and the STFC. Part of this work was carried out at the

Brookhaven National Laboratory which is operated for the U. S. Department of Energy by Brookhaven Science Associates (DE-AcO2-98CH10886).

[1] B. Lake, A. M. Tsvelik, S. Notbohm, D. A. Tennant, T. G. Perring, M. Reehuis, C. Sekar, G. Krabbes, and B. Buchner, Nat. Phys. **6**, 50 (2010).
[2] M. Greiter, Nat. Phys. **6**, 6 (2010).
[3] R. Loudon, *Quantum theory of light* (Oxford University Press, Oxford, 2001).
[4] P. W. Anderson, Science **235**, 1196 (2012).
[5] F. C. Zhang and R. M. Rice, Phys. Rev. B **37**, s759 (1988).
[6] K. B. Efetov, H. Meier, and C. Pepin, Nat. Phys. **9**, 442 (2013).
[7] C. Stock, C. Broholm, F. Demmel, J. V. Dujin, J. W. Taylor, H. J. Kang, R. Hu, and C. Petrovic, Phys. Rev. Lett. **109**, 127201 (2012).
[8] T. H. Hand, J. S. Helton, S. Y. Chu, D. G. Nocera, J. A. Rodriguez-Rivera, C. Broholm, and Y. S. Lee, Nature **492**, 406 (2012).
[9] M. A. de Vries, J. R. Stewart, P. P. Deen, J. O. Piatek, G. J. Nilsen, H. M. Ronnow, and A. Harrison, Phys. Rev. Lett. **103**, 237201 (2009).
[10] M. Fujita, H. Hiraka, M. Matsuda, M. Matsuura, J. M. Tranquada, S. Wakimoto, G. Xu, and K. Yamada, J. Phys. Soc. Jpn. **81**, 011007 (2012).
[11] M. A. Kastner, R. J. Birgeneau, G. Shirane, and Y. Endoh, Rev. Mod. Phys. **70**, 897 (1998).
[12] R. J. Birgeneau, C.Stock, J. M. Tranquada, and K. Yamada, J. Phys. Soc. Jpn. **75**, 111003 (2006).
[13] G. R. Stewart, Rev. Mod. Phys. **83**, 1589 (2011).
[14] J. Paglione and R. L. Greene, Nat. Phys. **6**, 645 (2010).
[15] D. C. Johnston, Adv. Phys. **59**, 803 (2010).
[16] W. Bao, P. G. Pagliuso, J. L. Sarrao, J. D. Thompson, Z. Fisk, J. W. Lynn, and R. W. Erwin, Phys. Rev. B **62**, R14621 (2000).
[17] W. Bao, G. Aeppli, J. W. Lynn, P. G. Pagliuso, J. L. Sarrao, M. F. Hundley, J. D. Thompson, and Z. Fisk, Phys. Rev. B **65**, 10050(R) (2002).
[18] S. Raymond, E. Ressouche, G. Knebel, D. Aoki, and J. Flouquet, J. Phys.: Condens. Matter **19**, 242204 (2007).
[19] G. F. Chen, K. Matsubayashi, S. Ban, K. Deguchi, and N. K. Sato, Phys. Rev. Lett. **97**, 017005 (2006).
[20] J. Paglione, P. C. Ho, M. B. Maple, M. A. Tanatar, L. Taillefer, Y. Lee, and C. Petrovic, Phys. Rev. B **77**, 100505(R) (2008).
[21] J. Paglione, M. A. Tanatar, D. G. Hawthorn, R. W. Hill, F. Ronning, M. Sutherland, L. Taillefer, C. Petrovic, and P. C. Canfield, Phys. Rev. Lett. **94**, 216602 (2005).
[22] K. Izawa, H. Yamaguchi, Y. Matsuda, H. Shishido, R. Settai, and Y. Onuki, Phys. Rev. Lett. **87**, 057002 (2001).
[23] H. Aoki, T. Sakakibara, H. Shishido, R. Settai, Y. Onuki, P. Miranovic, and K. Machida, J. Phys.: Condens. Matter **16**, L13 (2004).
[24] C. Stock, C. Broholm, Y. Zhao, F. Demmel, H. J. Kang, K. C. Rule, and C. Petrovic, Phys. Rev. Lett. **109**, 167207 (2012).
[25] C. Stock, C. Broholm, J. Hudis, H. J. Kang, and C. Petrovic, Phys. Rev. Lett. **100**, 087001 (2008).
[26] M. Kenzelmann, T. Strassle, C. Niedermayer, M. Sigrist, B. Padmanabham, M. Zolliker, A. D. Bianchi, R. Movshovich, E. D. Bauer, J. L. Sarrao, and J. D. Thompson, Science **321**, 1652 (2008).
[27] E. Blackburn, P. Das, M. R. Eskildsen, E. M. Forgan, M. Laver, C. Niedermayer, C. Petrovic, and J. S. White, Phys. Rev. Lett. **105**, 187001 (2010).
[28] C. Petrovic, P. G. Pagliuso, M. F. Hundley, R. Movshovich, J. L. Sarrao, J. D. Thompson, Z. Fisk, and P. Monthoux, J. Phys.: Condens. Matter **13**, L337 (2001).
[29] M. Blume, Phys. Rev. **130**, 1670 (1963).
[30] E. E. Rodriguez, C. Stock, K. L. Krycka, C. F. Majkrzak, P. Zajdel, K. Kirshenbaum, N. P. Butch, S. R. Saha, J. Paglione, and M. A. Green, Phys. Rev. B **83**, 134438 (2011).
[31] J. O. Dimmock, Phys. Rev. **130**, 1337 (1963).
[32] H. F. Franzen, Chem. Mater. **2**, 486 (1990).
[33] R. J. Birgeneau, H. J. Guggenheim, and G. Shirane, Phys. Rev. B **8**, 304 (1973).
[34] J. S. Kim, J. Alwood, D. Mixson, P. Watts, and G. R. Stewart, Phys. Rev. B **66**, 134418 (2002).
[35] T. Park, F. Ronning, H. Q. Yuan, M. B. Salamon, R. Movshovich, J. L. Sarrao, and J. D. Thompson, Nature **440**, 65 (2006).
[36] P. J. Brown, *International Tables of Crystallography, Vol C* (Kluwer, Dordrecht, 2006).
[37] A. D. Christianson, J. M. Lawrence, P. G. Pagliuso, N. O. Moreno, J. L. Sarrao, J. D. Thompson, P. S. Riseborough, S. Kern, E. A. Goremychkin, and A. H. Lacerda, Phys. Rev. B **66**, 193102 (2002).
[38] D. A. Tennant, T. G. Perring, R. A. Cowley, and S. E. Nagler, Phys. Rev. Lett. **70**, 4003 (1993).
[39] D. A. Tennant, R. A. Cowley, S. E. Nagler, and A. M. Tsvelik, Phys. Rev. B **52**, 13368 (1995).
[40] T. Huberman, R. Coldea, R. A. Cowley, D. A. Tennant, R. L. Lenheny, R. J. Christianson, and C. D. Frost, Phys. Rev. B **72**, 014413 (2005).
[41] I. U. Heilmann, J. K. Kjems, Y. Endoh, G. F. Reiter, G. Shirane, and R. J. Birgeneau, Phys. Rev. B **24**, 393 (1981).
[42] R. Coldea, S. M. Hayden, G. Aeppli, T. G. Perring, C. D. Frost, T. E. Mason, S. W. Cheong, and Z. Fisk, Phys. Rev. Lett. **86**, 5377 (2001).
[43] O. F. Sylijuasen and P. A. Lee, Phys. Rev. Lett. **88**, 207207 (2002).
[44] C. Stock, submitted.
[45] C. Stock, R. A. Cowley, W. J. L. Buyers, R. Coldea, C. Broholm, C. D. Frost, R. J. Birgeneau, R. Liang, D. Bonn, and W. N. Hardy, Phys. Rev. B **75**, 172510 (2007).
[46] C. Stock, R. A. Cowley, W. J. L. Buyers, C. D. Frost, J. W. Taylor, D. Peets, R. Liang, D. Bonn, and W. N. Hardy, Phys. Rev. B **82**, 174505 (2010).
[47] T. Timusk and B. Statt, Rep. Prog. Phys. **62**, 61 (1999).
[48] N. S. Headings, S. M. Hayden, R. Coldea, and T. G. Perring, Phys. Rev. Lett. **105**, 247001 (2010).